



HAL
open science

Thin Plasma Cavities as a Source of the Auroral Kilometric Radiation

T. M. Burinskaya, J. L. Rauch

► **To cite this version:**

T. M. Burinskaya, J. L. Rauch. Thin Plasma Cavities as a Source of the Auroral Kilometric Radiation. Planetary Radio Emissions VI, Apr 2005, Graz, Austria. pp.241-248. insu-03611264

HAL Id: insu-03611264

<https://insu.hal.science/insu-03611264>

Submitted on 17 Mar 2022

HAL is a multi-disciplinary open access archive for the deposit and dissemination of scientific research documents, whether they are published or not. The documents may come from teaching and research institutions in France or abroad, or from public or private research centers.

L'archive ouverte pluridisciplinaire **HAL**, est destinée au dépôt et à la diffusion de documents scientifiques de niveau recherche, publiés ou non, émanant des établissements d'enseignement et de recherche français ou étrangers, des laboratoires publics ou privés.

THIN PLASMA CAVITIES AS A SOURCE OF THE AURORAL KILOMETRIC RADIATION

T. M. Burinskaya* and J. L. Rauch†

Abstract

The investigation of the cyclotron maser instability in sources of finite perpendicular extension separated from the denser and cold surrounding plasma by sharp density gradients is made within the waveguide approximation. The general dispersion equation of wave propagation and amplification is obtained and solved numerically for different regimes. It is found that the growth rate of oblique eigenmode increases with the increasing of the perpendicular component of the wave vector directed along cavity boundaries. The structure of electromagnetic fields inside the source region is studied and changes of the wave polarization are discussed.

1 Introduction

Experimental data obtained during the modern spacecraft missions strongly suggest that Auroral Kilometric Radiation (AKR) sources have a small extension (usually not more than one hundred km) in the direction perpendicular to the geomagnetic field. AKR sources are observed as plasma cavities, filled by hot and tenuous plasma, and separated from the denser and colder surrounding plasma by sharp density gradient with typical scale length of the order or below 1 km. The electron population in these regions is dominated by particles with low parallel velocities and the energy of the order of several keV [Louarn and Le Quéau, 1996a]. During the last years it was established that the most likely mechanism for the generation of AKR, as well as to its analogs at other magnetized planets (Jupiter, Saturn and Uranus), is the electron cyclotron maser instability (CMI) [Wu and Lee, 1979; Pritchett 1984]. Louarn and Le Quéau [1996b] were the first who suggested a waveguide model for the AKR source, on the basis that a source boundary thickness is less than a typical wave length, whereas a source width is far in excess. They derived a dispersion equation for the waveguide eigenmode frequencies and solved it for different parameter regimes. However their results are correct for waves propagating along the magnetic field only. Since a waveguide model of the AKR source seems to us very promising in the light of the experimental data, we have found a dispersion equation of wave excitation and amplification in sources of finite extension in the general case.

* *Space Research Institute, Russian Academy of Sciences, Profsoyuznaya St. 84/32 Moscow, Russia*

† *CNRS LPCE, 3A, Avenue de la Recherche Scientifique, 45071 Orléans cedex 2, France*

2 Model and basic equations

The model of the AKR source region is chosen similar to [Louarn and Le Quéau, 1996b]. It is a slab structure limited in the x direction with width $L = 2l$ and unlimited in the y and z directions (z is along the background magnetic field in the opposite direction to it) (Fig.1). The source region is separated from the denser and cold surrounding plasma by infinitely density gradients. Inside the source the electron population consist of energetic particles with a ring-like distribution: $(f(v_z, v_\perp) = (2\pi v_{\perp 0})^{-1} \delta(v_\perp - v_{\perp 0}) \delta(v_z - v_0)$, where v_0 is an electron velocity along the background magnetic field. Although such a distribution

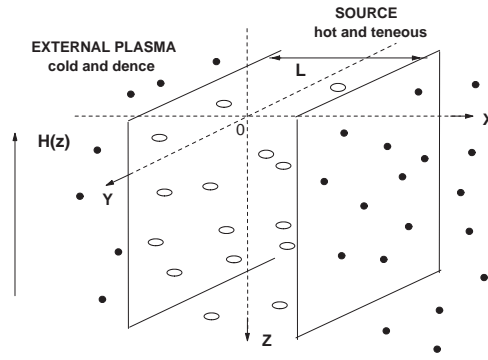


Figure 1: The model of the source region

is idealized, it takes into account relativistic effects and does not significantly modify the results obtained with the use of more realistic distributions as shown in [Pritchett 1984]. Assuming that changes of plasma parameters have a characteristic scale larger than a source width, the plasma inside and outside the source region may be considered as homogeneous. Writing the Maxwell equations with a appropriate dielectric tensor for each of the three homogeneous regions in the Fourier space, we perform a Fourier transform in the y and z directions:

$$\vec{\nabla} \times \vec{H} = -i \frac{\omega}{c} (\hat{\varepsilon} \vec{E}), \quad \vec{\nabla} \times \vec{E} = i \frac{\omega}{c} \vec{H}, \quad (1)$$

where c is a speed of light, $\vec{\varepsilon}$ is the dielectric tensor and $\vec{\nabla} = (\nabla_x, ik_y, ik_z)$. Since in the region of the AKR generation the electron plasma frequency (ω_p) is much less than the electron gyrofrequency (ω_c) and AKR wavelengths are much larger than the electron Larmor radius, it can be shown that for the ring-distribution the dielectric tensor components are the next:

$$\begin{aligned} \varepsilon_{xx} = \varepsilon_{yy} &\equiv \varepsilon_1, & \varepsilon_{zz} &= 1, \\ \varepsilon_{xy} = -\varepsilon_{yx} &\equiv \varepsilon_2, & \varepsilon_{xz} = \varepsilon_{yz} = \varepsilon_{zx} = \varepsilon_{zy} &= 0, \end{aligned} \quad (2)$$

where $\varepsilon_1 = \varepsilon_1^i$, $\varepsilon_2 = \varepsilon_2^i$ for the plasma inside a source region and $\varepsilon_1 = \varepsilon_1^0$, $\varepsilon_2 = \varepsilon_2^0$ for the outside plasma.

$$\begin{aligned}
\varepsilon_1^i &= 1 - \frac{\alpha_i}{2\omega^2}(F_1 + F_2), & \varepsilon_2^i &= \frac{\alpha_i}{2\omega^2}(F_1 - F_2) \\
F_1 &= \frac{\omega - N_z u_0}{\omega - 1 + \delta_\Sigma - N_z u_0} + \frac{v_\perp^2}{2c^2} \frac{N_z^2 - \omega}{(\omega - 1 + \delta_\Sigma - N_z u_0)^2}, \\
F_2 &= \frac{\omega - N_z u_0}{\omega + 1 - \delta_\Sigma - N_z u_0} + \frac{v_\perp^2}{2c^2} \frac{N_z^2 - \omega}{(\omega + 1 - \delta_\Sigma - N_z u_0)^2}, \\
\varepsilon_1^0 &= 1 - \frac{\alpha_0}{2\omega} \left(\frac{1}{\omega - 1} + \frac{1}{\omega + 1} \right), & \varepsilon_2^0 &= \frac{\alpha_0}{2\omega} \left(\frac{1}{\omega - 1} + \frac{1}{\omega + 1} \right),
\end{aligned} \tag{3}$$

where normalized parameters and variables are used: $\alpha_i = \omega_{pi}^2/\omega_c^2$, $\alpha_0 = \omega_{p0}^2/\omega_c^2$ (ω_{pi}, ω_{p0} are electron plasma frequencies inside and outside the source respectively), $\omega = \omega/\omega_c$, $N_z = k_z c/\omega_c$, $u_0 = v_0/c$, $\delta_\Sigma = (v_{\perp 0}^2 + v_0^2)/2c^2$. From equations (1), (2) all the components of the electromagnetic field can be written as functions of the parallel electric and magnetic field components only:

$$\begin{aligned}
H_x &= \frac{N_y E_z - N_z E_y}{\omega}, & H_y &= \frac{i}{\omega} \frac{\partial E_z}{\partial x} + \frac{N_z}{\omega} E_x, \\
E_x &= \frac{1}{D} \left\{ i N_z \left[\left(\varepsilon_1 - \frac{N_z^2}{\omega^2} \right) \frac{\partial E_z}{\partial x} + \varepsilon_2 N_y E_z \right] - \omega \left(\varepsilon_2 \frac{\partial H_z}{\partial x} + N_y \left(\varepsilon_1 - \frac{N_z^2}{\omega^2} \right) H_z \right) \right\}, \\
E_y &= -\frac{1}{D} \left\{ N_z \left[\varepsilon_2 \frac{\partial E_z}{\partial x} + \left(\varepsilon_1 - \frac{N_z^2}{\omega^2} \right) N_y E_z \right] + i \omega \left[- \left(\frac{N_z^2}{\omega^2} - \varepsilon_1 \right) \frac{\partial H_z}{\partial x} + \varepsilon_2 N_y H_z \right] \right\}, \\
D &= \omega^2 \left[\left(\varepsilon_1 - \frac{N_z^2}{\omega^2} \right)^2 - \varepsilon_2^2 \right],
\end{aligned} \tag{4}$$

where $N_y = k_y c/\omega_c$, $x = x\omega_c/c$. The parallel components of the electric and magnetic field are related by the equations:

$$\begin{aligned}
\frac{\partial^2 E_z}{\partial x^2} - \frac{N_y^2}{\omega^2} E_z + \left(1 - \frac{N_z^2}{\varepsilon_1 \omega^2} \right) E_z &= i \frac{N_z}{\omega} \frac{\varepsilon_2}{\varepsilon_1} H_z, \\
\frac{\partial^2 H_z}{\partial x^2} - \frac{N_y^2}{\omega^2} H_z + \left(\frac{\varepsilon_1^2 - \varepsilon_2^2}{\varepsilon_1} - \frac{N_z^2}{\omega^2} \right) H_z &= -i \frac{N_z}{\omega} \frac{\varepsilon_2}{\varepsilon_1} E_z
\end{aligned} \tag{5}$$

For the case of a perpendicular propagation ($N_z = 0$) the upper equation (6) describes the ordinary (O) mode and the bottom corresponds to the extraordinary (X) mode when $N_\perp^2 = (N_x^2 + N_y^2) < 1$ ($\omega^2/\omega_c^2 \approx 1$).

The general solution of equations (6) inside the AKR source is a superposition of two extraordinary and two ordinary mode waves. Thus for $-L/2 \leq x \leq L/2$

$$H_z^i = (a_1 \cos(N_1 x) + b_1 \sin(N_1 x) + a_2 \cos(N_2 x) + b_2 \sin(N_2 x)) \exp(i(N_y y + N_z z - \omega t)) \tag{7}$$

Outside the source the solution is

for $x > L/2$

$$H_z^+ = (A_1 \exp(iN_3(x - L/2)) + A_2 \exp(iN_4(x - L/2))) \exp(i(N_y y + N_z z - \omega t)),$$

for $x < -L/2$

$$H_z^- = (B_1 \exp(-iN_3(x + L/2)) + B_2 \exp(-iN_4(x + L/2))) \exp(i(N_y y + N_z z - \omega t)).$$

(8)

In expressions (7,8) N_1, N_3 are the transverse wave numbers for the X mode and N_2, N_4 for the O mode. For each of the three homogeneous regions transverse wave numbers are found from the dispersion equation with corresponding ε_1 and ε_2 :

$$\left(1 - \frac{N_z^2}{\varepsilon_1 \omega^2} - \frac{N_{\perp}^2}{\omega^2}\right) \left(\frac{\varepsilon_1^2 - \varepsilon_2^2}{\varepsilon_1} - \frac{N_z^2 + N_{\perp}^2}{\omega^2}\right) = \frac{N_z^2 \varepsilon_2^2}{\omega^2 \varepsilon_1^2} \quad (9)$$

The dispersion equation for the waveguide eigenmodes is found from the continuity of H_z , E_z , H_y and E_y .

3 Study of dispersion equation

3.1 Eigenmodes for the wave transverse propagation

First we consider the equation of wave propagation and amplification for $N_z = 0$. In this case the parallel electric and magnetic fields are decoupled and the electromagnetic field can be decomposed into waves corresponding to X ($E_z = 0$) or O ($H_z = 0$) modes. Thus in the general solution (7,8) we take into consideration only the terms attributing to X mode ($a_2 = b_2 = A_2 = B_2 = 0$). Substituting (7,8) into the expression for E_y (5) and using the conditions of continuity: $H_z^i = H_z^+$, $E_y^i = E_y^+$ for $x = L/2$ and $H_z^i = H_z^-$, $E_y^i = E_y^-$ for $x = -L/2$, the system of four linear equations is obtained. The compatibility conditions of this system gives the dispersion equation:

$$\begin{aligned} & \left\{ \frac{1}{D^i} [\varepsilon_1^i N_1 \sin(N_1 l) - \varepsilon_2^i N_y \cos(N_1 l)] + \frac{\cos(N_1 l)}{D^0} [i N_3 \varepsilon_1^0 + \varepsilon_2^0 N_y] \right\} \\ & \times \left\{ \frac{1}{D^i} [\varepsilon_1^i N_1 \cos(N_1 l) - \varepsilon_2^i N_y \sin(N_1 l)] - \frac{\sin(N_1 l)}{D^0} [i N_3 \varepsilon_1^0 - \varepsilon_2^0 N_y] \right\} \\ & = - \left\{ \frac{1}{D^i} [\varepsilon_1^i N_1 \sin(N_1 l) + \varepsilon_2^i N_y \cos(N_1 l)] + \frac{\cos(N_1 l)}{D^0} [i N_3 \varepsilon_1^0 - \varepsilon_2^0 N_y] \right\} \\ & \times \left\{ \frac{1}{D^i} [\varepsilon_1^i N_1 \cos(N_1 l) + \varepsilon_2^i N_y \sin(N_1 l)] - \frac{\sin(N_1 l)}{D^0} [i N_3 \varepsilon_1^0 + \varepsilon_2^0 N_y] \right\} \end{aligned} \quad (10)$$

Here D^i and D^0 are found with the use of (5) by substituting $\varepsilon_1^i, \varepsilon_2^i$ and $\varepsilon_1^0, \varepsilon_2^0$ respectively. Equation (10) depends on N_y^2 as it must be, because there is no difference for wave propagation in the positive or negative y direction. Contrary to this the dispersion equation (15) obtained in [Louarn and Le Quéau, 1996b] depends on N_y , because symmetric functions were chosen as solutions and the use of them is correct only for the case $N_y = 0$. The reason is that although the equation (6) for H_z may have symmetric ($b_1 = 0$) and antisymmetric ($a_1 = 0$) solutions, it is impossible for any of them to satisfy the boundary conditions for $x = -L/2$ and $x = L/2$ simultaneously, when $N_y \neq 0$. It follows from the fact that expression (5) for E_y , have terms with H_z and $\partial H_z / \partial x$ simultaneously.

Solutions of the dispersion equation for $N_y = 0$ were studied by Louarn and Le Quéau [1996b] in details and it was shown that each of the solutions can be labeled by an integer n . In this paper we determine $n \approx 1 + N_1 * L / \pi$ (here L is a normalized width $L = \omega_c L / c$) indicating the number of maximums of $|H_z|$ inside the source. We have studied the

numerical solutions of equation (10) depending on the value of N_y for different eigenmodes denoted by n . The normalized parameters used for calculations are similar to [Louarn and Le Quéau, 1996b]: $\alpha_i = 0.002, \alpha_0 = 0.01, u_0 = 0., \delta_\Sigma = 0.0075, l = \omega_c l / c = 60$. At an altitude where $f_c = 200 \text{ kHz}$ the width corresponds to $\approx 30 \text{ km}$, the internal density to $\approx 1 \text{ cm}^{-3}$, the external density to $\approx 5 \text{ cm}^{-3}$ and the electron energy $\approx 4 \text{ KeV}$. Solutions of (10) are plotted in Fig.2, where the normalized frequency represented by $\delta\omega = (\omega - \omega_c) / \omega_c$ and the growth rate $\gamma = \gamma / \omega_c$ are shown as a function of N_y for different n . As follows

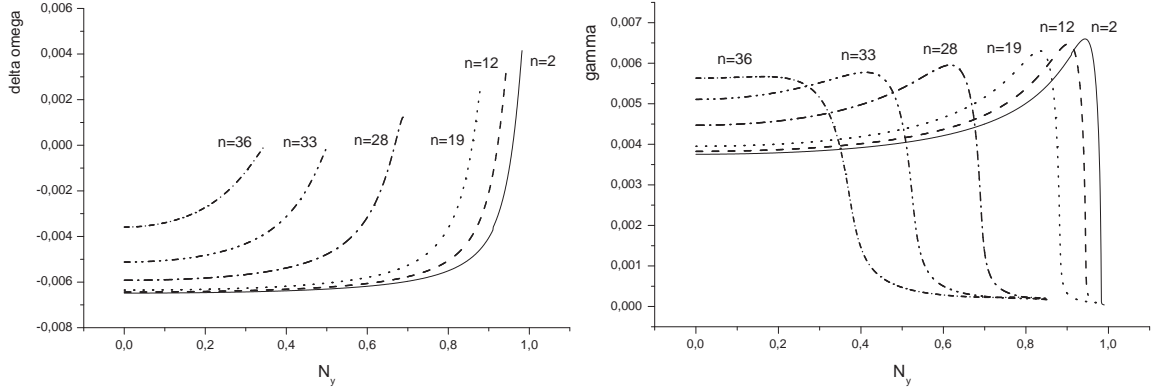


Figure 2: N_y - dependence of $\delta\omega$ and γ for different eigenmodes, $N_z = 0$

from numerical results the greater is the eigenmode number n , the less is an interval of N_y where the wave amplification is possible. Obviously it is a consequence of the X mode condition $N_1^2 + N_y^2 < 1$, because $n \approx 1 + N_1 * L / \pi$. It worth to note that the growth rate has the greater value for oblique eigenmodes with small number n . Taking into account the ratio between coefficients in the solution (7), following from the system of linear equations obtained for the derivation of dispersion equation (10),

$$\frac{b_1}{a_1} = \frac{\left\{ \frac{1}{D^i} [\varepsilon_1^i N_1 \sin(N_1 l) - \varepsilon_2^i N_y \cos(N_1 l)] + \frac{\cos(N_1 l)}{D^0} [i N_3 \varepsilon_1^0 + \varepsilon_2^0 N_y] \right\}}{\left\{ \frac{1}{D^i} [\varepsilon_1^i N_1 \cos(N_1 l) + \varepsilon_2^i N_y \sin(N_1 l)] - \frac{\sin(N_1 l)}{D^0} [i N_3 \varepsilon_1^0 + \varepsilon_2^0 N_y] \right\}}, \quad (11)$$

it is possible to illustrate the modification of the eigenmode in dimensionless units versus N_y . In Fig.3 the structure of $|H_z|$ for the eigenmode $n = 12$ ($N_1 = 0.289$) is shown for $N_y = 0$ (symmetric solution) and for $N_y = 0.5$ (asymmetric solution). The polarization of X mode for the case $N_y = 0$ is $|E_x| / |E_y| = \varepsilon_2 / \varepsilon_1 < 1$. Thus E_y dominates for the case $N_y = 0$ and $|E_x| / |E_y|$ is not dependent on the x coordinate inside the source. However with a growth of N_y the polarization becomes strongly coordinate dependent and the ratio $|E_x| / |E_y|$ may achieve high values. The structure of the polarization drastically changes for the case $N_y \neq 0$ as it is shown in Fig.4 for the eigenmode $n = 12$.

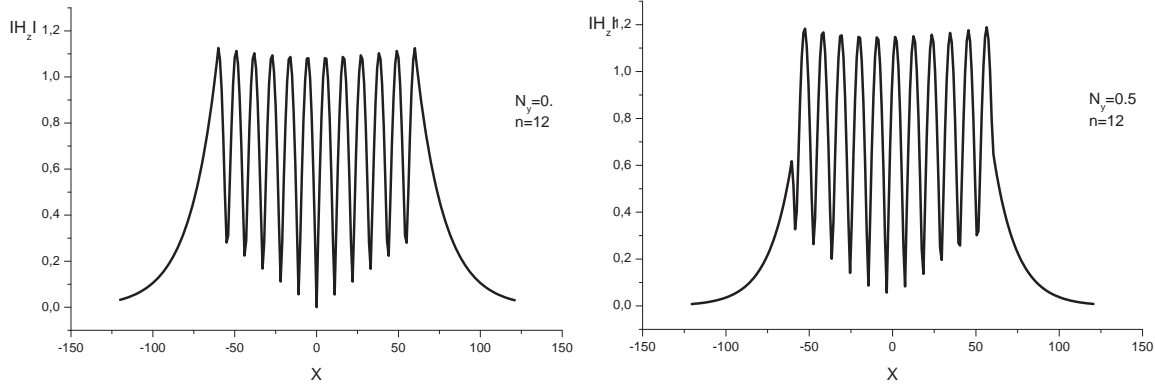


Figure 3: Structure of the $|H_z|$ for the eigenmode $n = 12$ for $N_y = 0$ and $N_y = 0.5$

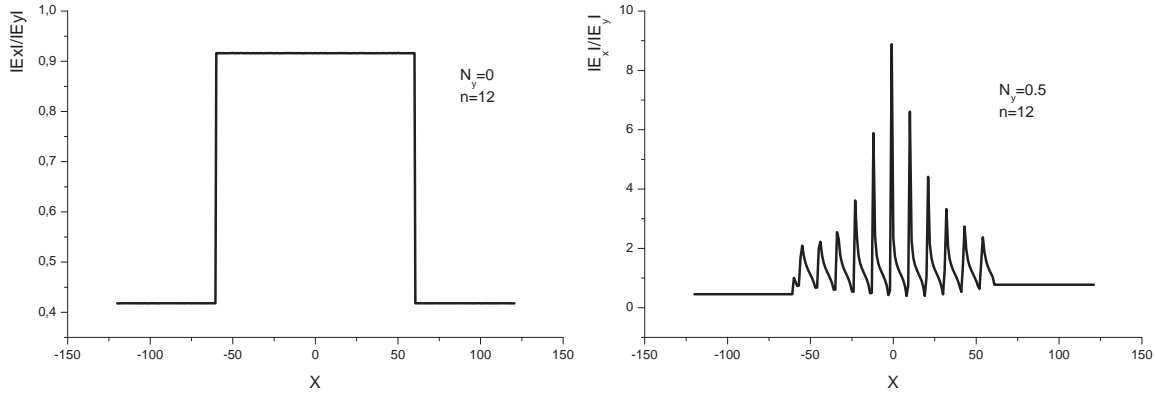


Figure 4: Polarization of the eigenmode $n = 12$ for $N_y = 0$ and $N_y = 0.5$

3.2 Eigenmodes for the wave propagation at an arbitrary angle to the magnetic field

In the waveguide approximation the dispersion equation for the wave propagation at an arbitrary angle to the background magnetic field is found by a routine way with a use of a general solution (7,8) and the continuity of H_z , E_z , H_y and E_y for $x = L/2$ and $x = -L/2$. Since this equation has a huge size, we do not reproduce it here but present some results obtained by numerical calculations. In [Louarn and Le Quéau, 1996b] the dependence of the dispersion equation upon N_z was obtained for $N_z \ll N_1$ but in our calculations we use the general dispersion equation for an arbitrary value of N_z without limitations.

In Fig. 5 the normalized frequency $\delta\omega = (\omega - \omega_c)/\omega_c$ and the growth rate $\gamma = \gamma/\omega_c$ are shown versus N_z for different n . A contraction of N_z range with the increasing of the eigenmode number is clearly seen. However the larger is the eigenmode number n , the greater is a value of the growth rate. Fig. 6 displays the N_z - dependence of the normalized frequency and growth rate for the eigenmode $n = 12$ for different N_y . As might be expected, there is a decreasing of N_z range with the increasing of N_y . Results of our investigation, when electrons velocity u_0 directed along the magnetic field inside the

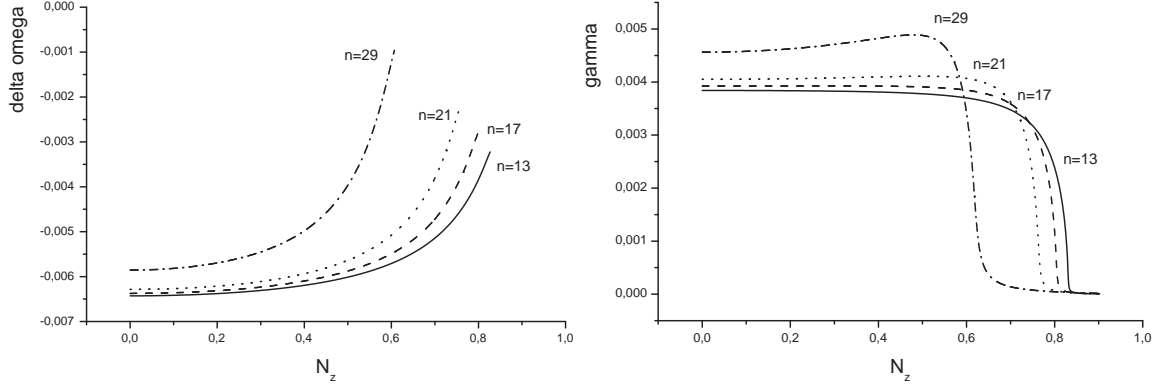


Figure 5: N_z - dependence of $\delta\omega$ and γ for different eigenmodes, $N_y = 0$

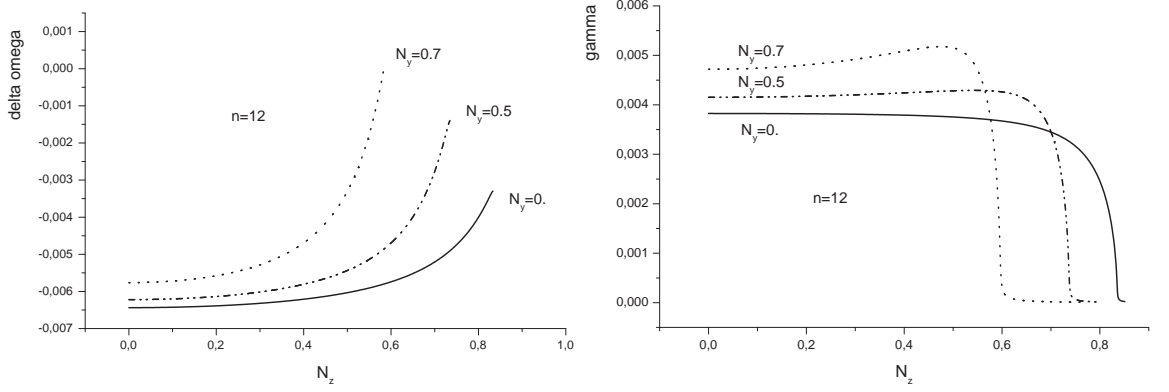


Figure 6: N_z - dependence of $\delta\omega$ and γ for the eigenmode $n = 12$ for different N_y

source region is taken into consideration, are plotted in Fig. 7 for the eigenmode $n = 29$ and different u_0 . For $u_0 \neq 0$ the N_z - dependence of the frequency is changed in such way that in the Earth magnetic field the waves generated with $N_z = 0$ or even having a rather small $N_z < 0$ directed from the Earth at first would propagate down to the Earth, because their group velocity $V_{gr} > 0$. After wave passing through the reflection point ($V_{gr} = 0$), waves propagate upward until they reach an altitude where the external X mode cut-off becomes equal to the wave frequency. Thus, although the N_z -dependence of the growth rate is practically the same (see Fig. 7) the wave amplification factor may increase due to the enhancement of wave duration inside the cavity.

4 Conclusion

The results of our investigation of the development of the CMI in sources of finite perpendicular extension in the waveguide approximation have shown that the growth rate of oblique eigenmode increases with the increasing of the perpendicular component of the wave vector directed along cavity boundaries. In general a structure of electromagnetic fields inside the source is asymmetric. E_y dominates for $N_y = 0$ and $|E_x|/|E_y|$ is not

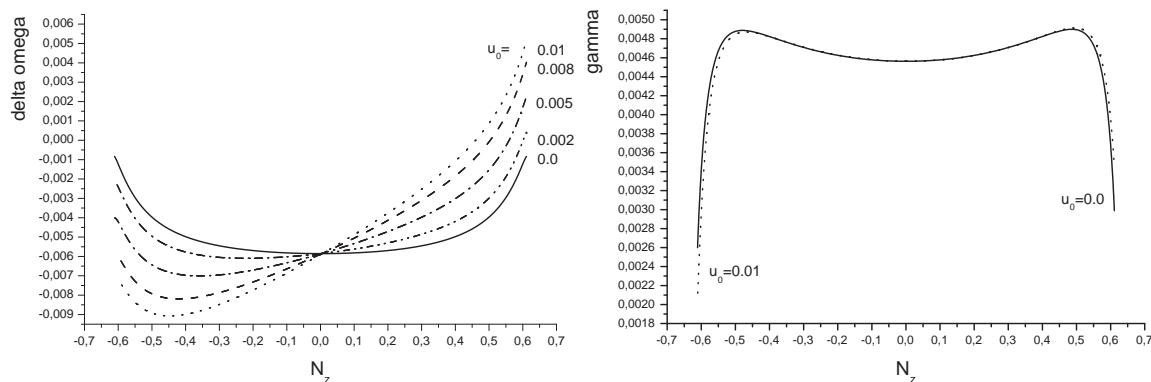


Figure 7: N_z - dependence of $\delta\omega$ and γ for the eigenmode $n = 29$ for different u_0

dependent on the coordinate inside the source. However with a growth of N_y the polarization becomes strongly coordinate dependent and the ratio $|E_x|/|E_y|$ may achieve high values in accordance with experimental observations.

Acknowledgments. This investigation was partially supported by grant of President RF HIII - 1739.2003.2 and RFBR grant 05-02-17566.

References

- Louarn, P., and D. Le Quéau, Generation of the Auroral Kilometric Radiation in plasma cavities: — I. Experimental study, *Planet. Space Sci.*, **44**, 199–210, 1996a.
- Louarn, P., and D. Le Quéau, Generation of the Auroral Kilometric Radiation in plasma cavities: - II. The cyclotron maser instability in small scale sources, *Planet. Space Sci.*, **44**, 211–224, 1996b.
- Pritchett, P. L., Relativistic dispersion, the cyclotron maser instability and auroral kilometric radiation, *J. Geophys. Res.*, **89**, 8957, 1984.
- Wu, C. S., and L. C. Lee, A theory of terrestrial kilometric radiation, *Astrophys. J.*, **230**, 621–626, 1979.